

# Controlled dispersion of a porphyrin/fullerene donor–acceptor complex in semiconducting polymer thin films: Intermolecular interactions of polymers with porphyrin and fullerene

Itaru Natori,<sup>1,2</sup> Shizue Natori,<sup>2</sup> Naoki Hanawa,<sup>2</sup> Kenji Ogino<sup>2</sup>

<sup>1</sup>Energy & Environment R&D Center, Corporate Research & Development, Asahi Kasei Corporation, 2-1 Samejima, Fuji City Shizuoka 416-8501, Japan

<sup>2</sup>Chemical and Material Systems, Graduate School of Bio-Applications and Systems Engineering, Tokyo University of Agriculture & Technology, 2-24-16 Naka-Chou, Koganei City, Tokyo 184-8588, Japan

Correspondence to: I. Natori (E-mail: itaru\_natori@yahoo.co.jp)

**ABSTRACT:** Thin films composed of semiconducting polymers [poly(2-vinyl naphthalene), poly(4-diphenyl aminostyrene), poly(1-vinyl pyrene), and poly(3-hexyl thiophene-2,5-diyl)], zinc(II)–5,10,15,20-*tetra*-(2-naphthyl)porphyrin, and [6,6]-phenyl-C<sub>61</sub>-butyric acid methyl ester blends were prepared to investigate the controlled dispersion of porphyrin molecules in semiconducting polymer thin films. Tailoring the intermolecular interactions between the polymer/fullerene, polymer/porphyrin, and porphyrin/fullerene systems was found to be an effective method of controlling the dispersion. When the polymer/porphyrin interactions were enhanced, intermixed porphyrin/fullerene donor–acceptor complex domains were formed, whereas under conditions where the polymer/porphyrin interactions were weakened, the complex assembled at the borders between the polymer and fullerene phases. This concept could potentially be applied to various combinations of porphyrin/fullerene systems in semiconducting polymer thin films to develop polymer solar cells with excellent performance. © 2014 Wiley Periodicals, Inc. *J. Appl. Polym. Sci.* **2015**, *132*, 41629.

**KEYWORDS:** blends; compatibilization; conducting polymers; films; optical and photovoltaic applications

Received 31 July 2014; accepted 12 October 2014

DOI: 10.1002/app.41629

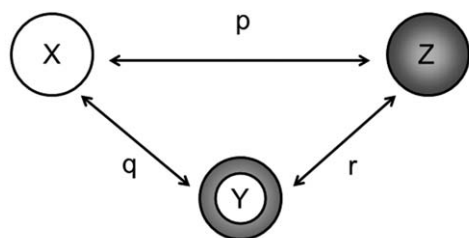
## INTRODUCTION

Among various donor–acceptor systems, the porphyrin (electron donor)/fullerene (electron acceptor) donor–acceptor complex has attracted much attention<sup>1–7</sup> because of its significant potential as a key component of polymer solar cells (PSCs).<sup>8–15</sup> These two compounds are stable, ecofriendly, inexpensive, and lightweight, and they have applications in flexible large-area devices. As a result, there have been many studies concerning the development of new PSCs consisting of a semiconducting polymer together with porphyrin and fullerene. However, previous attempts to incorporate porphyrins into PSCs have resulted in limited success because of the difficulty in controlling the dispersion of porphyrin molecules into polymer thin films. Therefore, new methods for controlling the dispersion of porphyrin/fullerene donor–acceptor complexes throughout semiconducting polymer thin films are required.

Recently, we proposed the tuning of the molecular compatibilities (i.e., intermolecular interactions) of polymer/fullerene, polymer/porphyrin, and porphyrin/fullerene (Scheme 1) systems as a new concept for the controlled dispersion of porphyrin

molecules into polymer thin films.<sup>16–18</sup> For example, when polycyclohexane (PCHE; a hydrocarbon polymer), zinc(II)–5,10,15,20-*tetra*-(2-naphthyl)porphyrin (ZnTNpP; a porphyrin derivative), and [6,6]-phenyl-C<sub>61</sub>-butyric acid methyl ester (PCBM; a fullerene derivative) were blended, a clear microphase separation of PCHE and PCBM was observed, and a ZnTNpP/PCBM donor–acceptor complex layer was formed between the PCHE and PCBM phases.<sup>18</sup> Furthermore, we have demonstrated the ready formation of porphyrin/fullerene donor–acceptor complexes in various polymer thin films, in which the intermolecular interactions caused by charge-transfer from porphyrin to fullerene within the porphyrin/fullerene complex appear to be very strong.<sup>16–18</sup> In addition, we noticed that the tracking location of maxima of the Soret band of porphyrin acted as a good indicator to reveal the degree of its aggregation in polymer/porphyrin blends. Therefore, we thought this to be an effective method for examining the molecular compatibility of polymers and porphyrin/fullerene donor–acceptor complexes.

Our subsequent work has focused on the application of this concept to the realization of the controlled dispersion of porphyrin molecules throughout semiconducting polymer/



X = Polymer      Y = Porphyrin      Z = Fullerene

p, q, r = Intermolecular Interaction

**Scheme 1.** Intermolecular interactions between polymer/fullerene (p), polymer/porphyrin (q), and porphyrin/fullerene (r).

porphyrin/fullerene blend thin films. For this purpose, several semiconducting polymers having different polymer-chain structures [poly(2-vinyl naphthalene (PVNP)), poly(4-diphenyl aminostyrene) (PDAS), and poly(1-vinyl pyrene) (PVPY)] were synthesized by (living) anionic polymerization. In addition, various combinations of these semiconducting polymers, PVNP, PDAS, PVPY, or poly(3-hexyl thiophene-2,5-diyl) (P3HT), were blended with ZnTNpP and PCBM (Scheme 2) to investigate the controlled dispersion of porphyrin molecules.

In this article, we report the controlled dispersion of porphyrin molecules in the form of porphyrin/fullerene donor–acceptor complexes into semiconducting polymer/porphyrin/fullerene blend thin films. The strengths of the intermolecular interactions between the semiconducting polymers, porphyrin, and fullerene are also discussed in detail.

## EXPERIMENTAL

### Materials

Toluene ( $\geq 99.8\%$ ), *N,N,N',N'*-tetramethyl ethylenediamine (TMEDA;  $\geq 99.5\%$ ), and tetrahydrofuran (THF;  $\geq 99.9\%$ ) were refluxed over calcium hydride ( $\text{CaH}_2$ ; 95%) and then distilled under dry argon. Methyl triphosphonium bromide ( $\geq 98.0\%$ ), 2-naphthaldehyde (NPA;  $\geq 98.0\%$ ), 4-(diphenylamino)benzaldehyde (DBA;  $\geq 98.0\%$ ), and 1-pyrenecarboxaldehyde (PYA;  $\geq 98.0\%$ ) were dried under reduced pressure. The monomers 2-vinyl naphthalene (2-VNP),<sup>19</sup> 4-diphenyl aminostyrene (4-DAS),<sup>20</sup> and 1-vinyl pyrene (1-VPY)<sup>21,22</sup> were synthesized from NPA, DBA, and PYA via standard Wittig reactions, which generated 2-VNP, 4-DAS, and 1-VPY at 92–93% yields. ZnTNpP was prepared according to a procedure previously described in the literature.<sup>23,24</sup> Other reagents were used as received unless otherwise stated. Methyl triphosphonium bromide, NPA, DBA, and PYA were purchased from Tokyo Chemical, whereas all other reagents were purchased from Sigma-Aldrich.

### General Procedure for the (Living) Anionic Polymerization of Vinyl Monomers with the Benzyl Lithium (BzLi)/TMEDA System<sup>20</sup>

A well-dried 50-mL Schlenk tube was purged with dry argon, and 5.0 mL of toluene was injected at room temperature (ca.

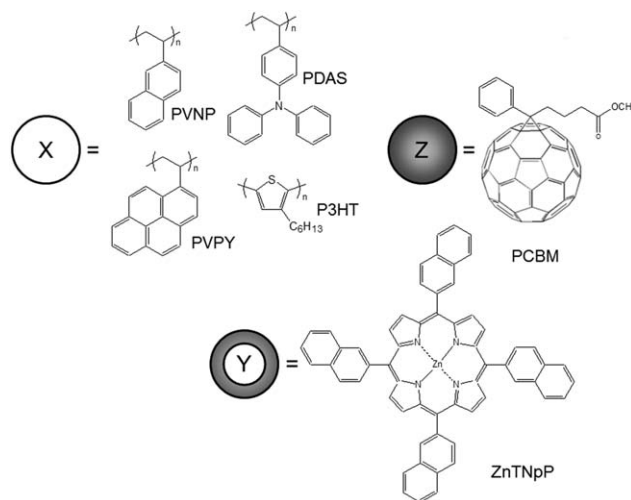
25°C) with a syringe. *t*-Butyl lithium (1.70M in pentane) was subsequently added to the tube with a syringe followed by the addition of TMEDA under dry argon; after this, the mixture was stirred for 10 min to generate the BzLi/TMEDA (1.00/1.25) system.<sup>20</sup> A toluene solution of the desired monomer (monomer/toluene = 0.50 g:5.00 mL) was added to this solution, and the reaction mixture was magnetically stirred under dry argon at room temperature. To terminate the reaction after polymerization, dry methanol (MeOH) was injected into the mixture in an amount equimolar to the quantity of lithium (Li) atoms present in the solution. The mixture was then poured into a large volume of MeOH to precipitate the polymer; this was subsequently separated by filtration. The product was dried under reduced pressure at room temperature for 24 h; this resulted in a white powdery polymer.

### Preparation of Polymeric Thin Films

Polymeric thin films were formed by the dissolution of each sample in chlorobenzene at a sample concentration of 10.0 mg/g and the spin coating of the solutions onto glass substrates at 2000 rpm (Mikasa, 1H-D3). The thicknesses of the resulting films, as measured with atomic force microscopy (AFM; JEOL JSPM-4200), were in the range 80–100 nm.

### Measurements

The number-average molecular weight ( $M_n$ ), weight-average molecular weight ( $M_w$ ), and polydispersity index (PDI;  $M_w/M_n$ ) of each polymer were determined with gel permeation chromatography instrumentation equipped with a differential refractive index detector and a Shimadzu Shim-Pack GPC-80M column (column length = 300 mm, diameter = 8 mm, effective molecular weight range = 100–4,000,000) at 40°C. THF was used as the eluent at a flow rate of 1.00 mL/min. A molecular weight calibration curve was obtained with polystyrene standards. The proton nuclear magnetic resonance (<sup>1</sup>H-NMR; JEOL ECA500) spectra of the polymers were acquired in deuterated chloroform ( $\text{CDCl}_3$ ) at 500 MHz. Ultraviolet–visible (UV–vis) absorption spectra of polymer sample solutions and films were obtained with a spectrometer (Shimadzu UV-3101PC). Photoluminescence (PL)



**Scheme 2.** Chemical structures of (X) the semiconducting polymers (PVNP, PDAS, PVPY, and P3HT), (Y) ZnTNpP, and (Z) PCBM.

**Table I.** Syntheses of PVNP, PDAS, and PVPY with the BzLi/TMEDA System as an Initiator<sup>a</sup>

Polymer	Initiator system (Li/TMEDA; mol/mol)	Monomer	[Monomer] <sub>0</sub> /[Li] <sub>0</sub>	Yield (wt %)	<i>M<sub>n</sub></i> (g/mol)	PDI
PVNP	BzLi/TMEDA (1.00:1.25)	2-VNP	13.0:1.00	87	1850	1.16
PDAS	BzLi/TMEDA (1.00:1.25)	4-DAS	7.40:1.00	100	1650	1.15
PVPY	BzLi/TMEDA (1.00/1.25)	1-VPY	8.76:1.00	92	2210	1.57

<sup>a</sup>Polymerization was performed in toluene (10.0 mL) under dry argon at room temperature for 3 h. Toluene/BzLi=10.0 mL:0.25 mmol.

spectra of the polymers were acquired in THF with a Jasco FP-777 spectrofluorometer with quartz cells. The extent of micro-phase separation of the polymer films was observed with AFM (JEOL JSPM-4200).

## RESULTS AND DISCUSSION

### Synthesis of PVNP, PDAS, and PVPY with the BzLi/TMEDA System as an Initiator

As we reported previously,<sup>20,25</sup> the BzLi/TMEDA (1.00/1.25) system is an excellent initiator system for the anionic polymerization of 4-DAS (a vinyl monomer containing several aromatic groups). The first successful example of the living anionic polymerization of 4-DAS was achieved with this initiator system.<sup>20</sup> Therefore, we anticipated that this initiator system would also be capable of polymerizing other vinyl monomers with multiple aromatic groups, such as 2-VNP and 1-VPY, so the anionic polymerization of these monomers was attempted under dry argon for 3 h in addition to the living anionic polymerization of 4-DAS under the same conditions.<sup>20</sup> The results obtained are summarized in Table I.

When each monomer solution was added to the BzLi/TMEDA system, a dark red coloration was observed because of the presence of the anion when either 2-VNP or 4-DAS was used, whereas 1-VPY generated a dark blue color. The 1-VPY polymerization system also appeared to be somewhat heterogeneous. After 3 h of reaction time, all three monomer systems generated polymeriza-

tion products. The yields of PVNP, PDAS, and PVPY were 87, 100, and 92 wt %, whereas the corresponding *M<sub>n</sub>* (PDI) values were 1850 (1.16), 1650 (1.15), and 2210 (1.57; Table I).

Figure 1 shows typical <sup>1</sup>H-NMR spectra obtained for PVNP, PDAS, and PVPY synthesized with the BzLi/TMEDA (1.00/1.25) system in toluene. In the case of PVNP [Figure 1(a)], the peaks from 6.0 to 8.0 ppm (Ha) were assigned to the aromatic protons on the naphthyl groups, whereas the peaks from 1.2 to 2.6 ppm (Hb) were assigned to the methine and methylene protons, respectively. With regard to PDAS [Figure 1(b)], the peaks from 6.5 to 7.5 ppm (Hc) were assigned to the aromatic protons on the triphenylamino groups, whereas those in the range from 1.2 to 2.5 ppm (Hd) were attributed to methine and methylene protons. In the PVPY spectrum [Figure 1(c)], the peaks from 5.8 to 8.5 ppm (He) were assigned to the aromatic protons on the pyrenyl groups, whereas the peaks from 0.8 to 2.8 ppm (Hf) were due to methine and methylene protons.

### Relationship Between the Degree of Aggregation and the Optical Properties of ZnTNpP

As reported in a previous article,<sup>18</sup> the optical properties of ZnTNpP were strongly influenced by the state of the molecules. In the UV-vis spectra, the Soret band of ZnTNpP was shifted to longer wavelengths with increasing degrees of aggregation, and so the degree of aggregation of ZnTNpP in the polymer thin film was examined by the assessment of the extent of the redshift of the Soret band (Scheme 3). As shown in Figure 2,<sup>18</sup> in the case of free ZnTNpP molecules (e.g., in a 0.00150 mg/mL THF solution), the Soret band was observed at 429 nm (line X). In contrast, when all of the ZnTNpP molecules were in direct contact,

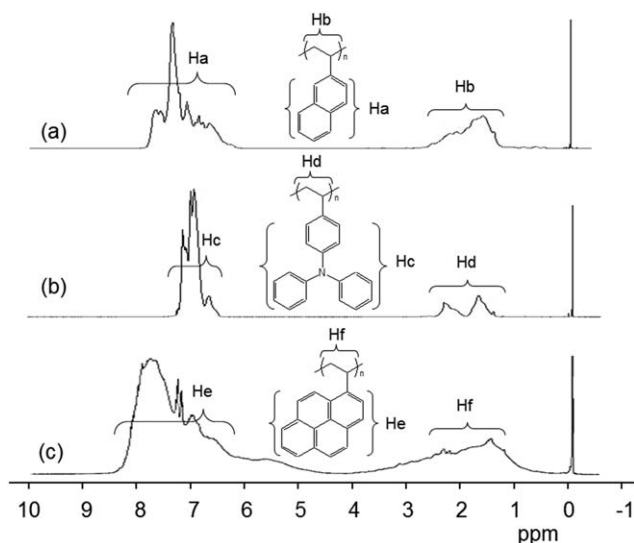
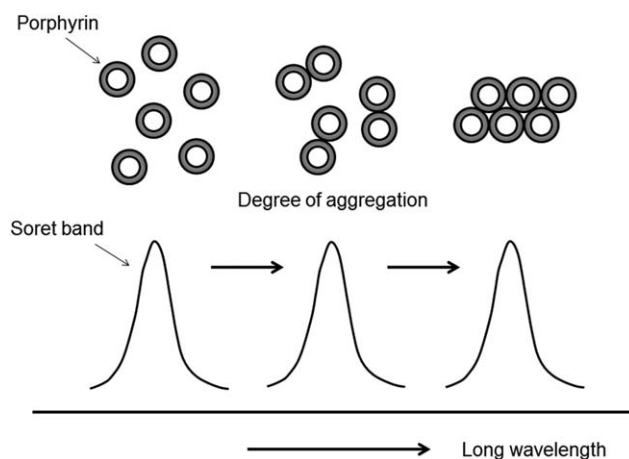


**Figure 1.** <sup>1</sup>H-NMR spectra of 3.0 wt % solutions of (a) PVNP (*M<sub>n</sub>* = 1850 g/mol, PDI = 1.16), (b) PDAS (*M<sub>n</sub>* = 1650 g/mol, PDI = 1.15), and (c) PVPY (*M<sub>n</sub>* = 2210 g/mol, PDI = 1.57) in CDCl<sub>3</sub> at 50°C.



**Scheme 3.** Relationship between the degree of aggregation and the Soret band in the UV-vis spectra of ZnTNpP.

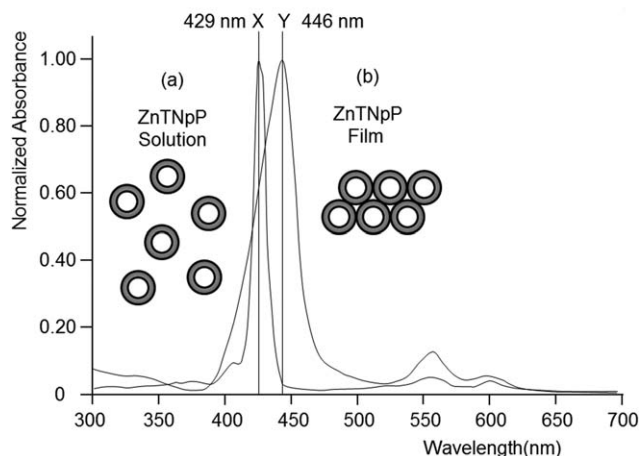


**Figure 2.** Normalized UV-vis spectra of (a) a 0.00150 mg/mL ZnTNpP solution in THF and (b) a ZnTNpP thin film prepared from a 10.0 mg/g chlorobenzene solution.

as in the spin-coated thin film, the Soret band was observed at 446 nm (line Y). The bands at about 570 and 600 nm corresponded to the Q bands of the ZnTNpP. It was, therefore, possible to determine the degree of aggregation of the ZnTNpP in a semiconducting polymer thin film (i.e., the degree of intermolecular interactions between the semiconducting polymer and the ZnTNpP) by tracking the location of the maxima of the Soret band observed in the region between 429 and 446 nm.

#### Effects of the Polymer Chain Structure on the Polymer/Porphyrin Intermolecular Interactions

To examine the intermolecular interactions between the semiconducting polymer and the ZnTNpP, a series of semiconducting polymer/ZnTNpP/PCBM blends were prepared in chlorobenzene [semiconducting polymer/ZnTNpP/PCBM = 60/40/0, 60/30/10, 60/20/20, and 60/10/30 w/w] at a sample/solvent ratio of 10.0 mg/g. Thin films of these blends were fabricated by the spin coating of the chlorobenzene solutions onto glass

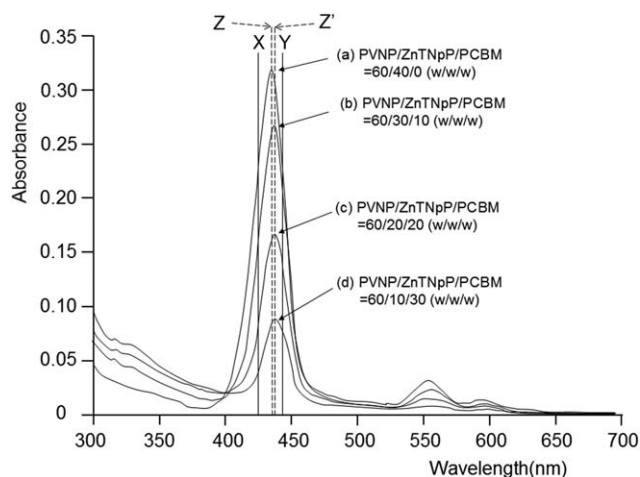


**Figure 3.** UV-vis spectra of the (a) 60/40/0 w/w PVNP/ZnTNpP/PCBM, (b) 60/30/10 PVNP/ZnTNpP/PCBM, (c) 60/20/20 PVNP/ZnTNpP/PCBM, and (d) 60/10/30 PVNP/ZnTNpP/PCBM blend thin films.

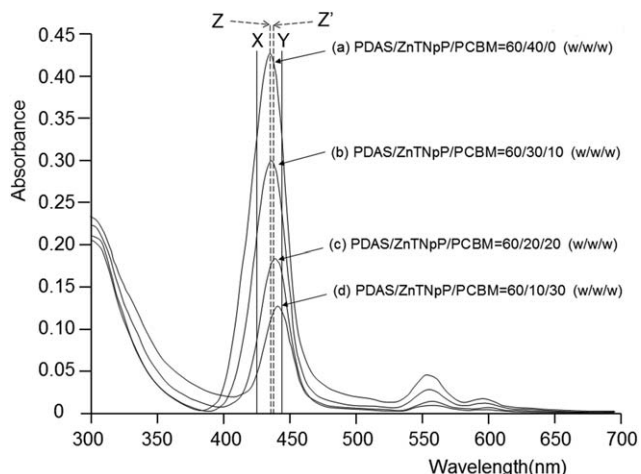


**Figure 4.** UV-vis spectra of the (a) 60/40/0 w/w PDAS/ZnTNpP/PCBM, (b) 60/30/10 PDAS/ZnTNpP/PCBM, (c) 60/20/20 PDAS/ZnTNpP/PCBM, and (d) 60/10/30 PDAS/ZnTNpP/PCBM blend thin films.

substrates, the UV-vis spectra of the thin films were acquired, and the results displayed in Figures 3–6.

Figure 3 presents the typical UV-vis spectra acquired for the PVNP/ZnTNpP/PCBM blend thin films. The Soret band for the 60/40/0 blend film [Figure 3(a)], which was initially close to the 429 nm value observed for pure ZnTNpP (line X; Figure 2), was observed to have shifted to a longer wavelength (line Z, ~440 nm) because of the slight self-aggregation of the ZnTNpP molecules in the PVNP thin film. When PCBM was added to the blend, the Soret band was shifted to somewhat longer wavelengths because of the increased aggregation of ZnTNpP molecules accompanying the formation of a ZnTNpP/PCBM donor-acceptor complex. However, the Soret bands of the 60/30/10, 60/20/20, and 60/10/30 blend films [Figures 3(b–d)] remained at approximately 442 nm (line Z').

Figure 4 shows the typical UV-vis spectra acquired for the PDAS/ZnTNpP/PCBM blend thin films. The Soret band for the 60/40/0 blend film, which was initially close to the 429 nm value of the pure ZnTNpP (line X; Figure 2), was shifted to a longer wavelength (line Z, about 440 nm) because of the slight self-aggregation of the ZnTNpP molecules in the PDAS thin film; this was similar to the behavior of the PVNP thin film. When PCBM was added to the blend, the Soret band was gradually shifted to longer wavelengths by the increase in the aggregation of ZnTNpP molecules that resulted from the formation of a ZnTNpP/PCBM donor-acceptor complex; the Soret band of the 60/10/30 blend film was shifted to approximately 444 nm.

Figure 5 provides the typical UV-vis spectra acquired for the PVPY/ZnTNpP/PCBM blend thin films. Here, the Soret band of the 60/40/0 blend film, which formerly appeared in the vicinity of the 429 nm value observed for pure ZnTNpP (line X; Figure 2), was shifted to a longer wavelength (line Z', about 442 nm) because of the minimal self-aggregation of ZnTNpP molecules in the PVPY thin film; this occurred to a somewhat greater extent than in the PVNP thin film. When PCBM was added to the blend, the Soret band was somewhat shifted to longer wavelengths by the increased aggregation of the

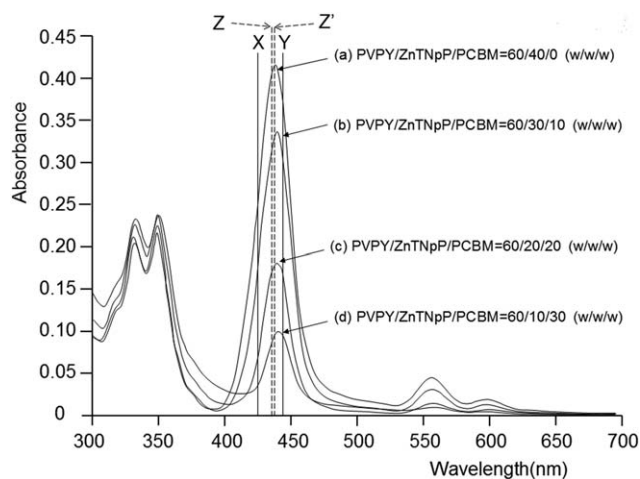


**Figure 5.** UV-vis spectra of the (a) 60/40/0 w/w PVPY/ZnTNpP/PCBM, (b) 60/30/10 PVPY/ZnTNpP/PCBM, (c) 60/20/20 PVPY/ZnTNpP/PCBM, and (d) 60/10/30 PVPY/ZnTNpP/PCBM blend thin films.

ZnTNpP molecules associated with the formation of a ZnTNpP/PCBM donor-acceptor complex. The Soret band of the 60/10/30 blend film shifted to approximately 444 nm; this was similar to the shift seen with the PDAS thin film.

Figure 6 shows the typical UV-vis spectra acquired for the P3HT/ZnTNpP/PCBM blend thin films. Here, the Soret band for the 60/40/0 blend film, which was initially close to the 429 nm value seen with the pure ZnTNpP (line X; Figure 2), was shifted to a longer wavelength (line Z', ~442 nm), once again because of some degree of self-aggregation of ZnTNpP molecules in the P3HT thin film and similar to the behavior of the PVPY thin film. When PCBM was added to the blend, the Soret band was shifted to even longer wavelengths by the increased aggregation of ZnTNpP molecules that accompanied the formation of a ZnTNpP/PCBM donor-acceptor complex. The Soret band of the 60/10/30 blend film was observed to shift to approximately 446 nm (line Y) because of the direct contact of all of the ZnTNpP molecules in this system.

From the results shown in Figures 2–6, we confirmed that the compatibility of the semiconducting polymer and ZnTNpP was evaluated by the tracking of the location of the maxima of the Soret band. On the basis of these results, the degree of aggregation of the ZnTNpP molecules in the semiconducting polymer blend films increased in the order PVNP/ZnTNpP/PCBM < PDAS/ZnTNpP/PCBM < PVPY/ZnTNpP/PCBM < P3HT/ZnTNpP/PCBM. Therefore, the strength of the intermolecular interactions between the polymer and the porphyrin (Scheme 1) decreased in the order PVNP/ZnTNpP > PDAS/ZnTNpP > PVPY/ZnTNpP > P3HT/ZnTNpP. Among the various combinations examined, both PVNP and ZnTNpP contain the same naphthalene moiety, and this similarity in their molecular structures may have explained the particularly strong intermolecular interactions in this system.

#### Intermolecular Interactions Between Porphyrin and Fullerene

As noted, the combination of PVNP and ZnTNpP exhibited the strongest intermolecular interactions in this study. Accordingly, the ZnTNpP molecules seemed to have been well dispersed

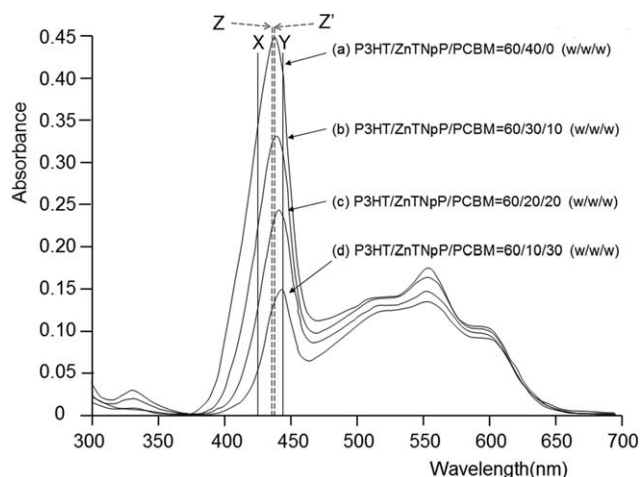
throughout the PVNP phase, even though excess PCBM molecules were added in the blend, as in the 60/10/30 PVNP/ZnTNpP/PCBM blend [Figure 3(d)]. In such cases, when the strength of the intermolecular interactions between the ZnTNpP and the PCBM was sufficiently strong compared to that between the PVNP/PCBM and PVNP/ZnTNpP, one would expect that all of the ZnTNpP molecules would be dispersed in the PVNP phase in the form of ZnTNpP/PCBM donor-acceptor complexes.<sup>16–18</sup> To examine the strengths of the intermolecular interactions of the porphyrin/fullerene system in the PVNP/ZnTNpP/PCBM blend, the PL spectra of the polymer thin films were acquired.

Figure 7 shows typical PL spectra obtained for the 90/10/0 and 60/10/30 PVNP/ZnTNpP/PCBM blend thin films. An emission peak around 620 nm was observed in the PL spectrum of the 90/10/0 blend film. When PCBM was added to form the 60/10/30 blend film, this emission peak was completely quenched. Therefore, the ZnTNpP and C<sub>60</sub> in the PCBM of the 60/10/30 blend film were believed to form a ZnTNpP/PCBM donor-acceptor complex because of the direct contact of all of the ZnTNpP and PCBM molecules, which resulted from the very strong intermolecular interactions between ZnTNpP and PCBM.

From these results, the intermolecular interactions in the porphyrin/fullerene system were thought to be much stronger than those in the polymer/fullerene and polymer/porphyrin systems; this reconfirmed that the porphyrin/fullerene donor-acceptor complex readily formed in the semiconducting polymer/porphyrin/fullerene blend film.

#### Dispersion State of the ZnTNpP/PCBM Donor-Acceptor Complex in the Polymer Thin Films

To examine the dispersion states of the ZnTNpP/PCBM donor-acceptor complex in the semiconducting polymer thin films, the extent of microphase separation of each blend film was observed by AFM. Figure 8 presents AFM images of the 60/10/30 PVNP/ZnTNpP/PCBM [Figure 8(a)], PDAS/ZnTNpP/PCBM [Figure 8(b)], PVPY/ZnTNpP/PCBM [Figure 8(c)], and P3HT/ZnTNpP/PCBM [Figure 8(d)] blend films. On the basis of the



**Figure 6.** UV-vis spectra of the (a) 60/40/0 w/w P3HT/ZnTNpP/PCBM, (b) 60/30/10 P3HT/ZnTNpP/PCBM, (c) 60/20/20 P3HT/ZnTNpP/PCBM, and (d) 60/10/30 P3HT/ZnTNpP/PCBM blend thin films.

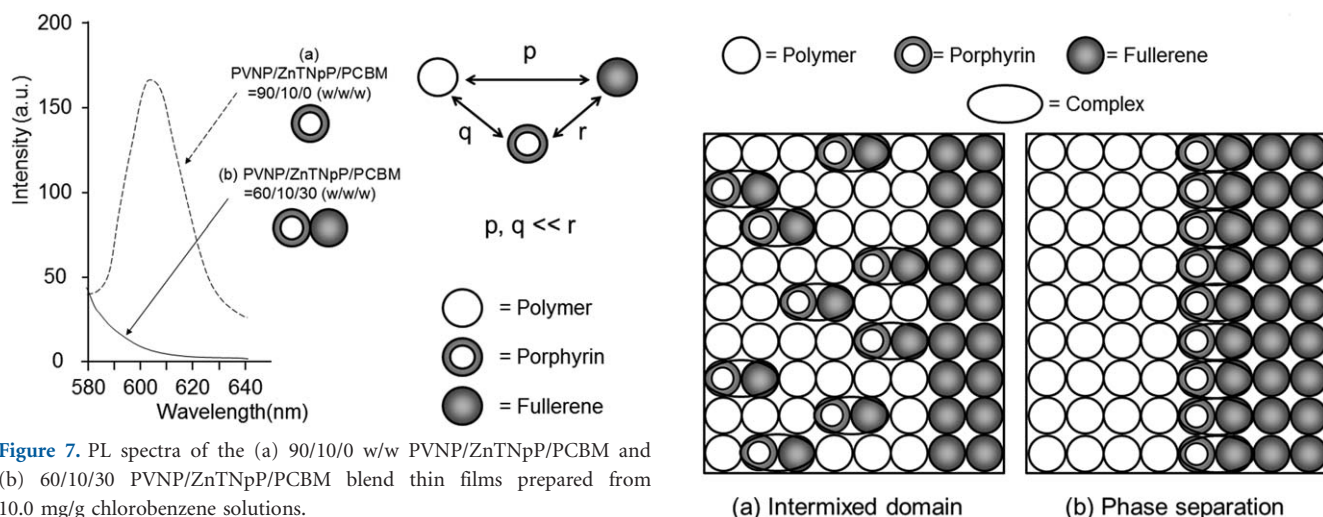


**Figure 7.** PL spectra of the (a) 90/10/0 w/w PVNP/ZnTNpP/PCBM and (b) 60/10/30 PVNP/ZnTNpP/PCBM blend thin films prepared from 10.0 mg/g chlorobenzene solutions.

results of our previous studies, the bright and dark regions in these images correspond to the polymer and PCBM phases, respectively.<sup>16–18</sup>

As shown in Figure 8, the microphase separation in the polymer thin films became more distinct in the order PVNP/ZnTNpP/PCBM [Figure 8(a)], PDAS/ZnTNpP/PCBM [Figure 8(b)],

**Scheme 4.** Controlled dispersion of the porphyrin/fullerene donor–acceptor complexes: (a) intermixed domains and (b) phase separation.

PVPY/ZnTNpP/PCBM [Figure 8(c)], and P3HT/ZnTNpP/PCBM [Figure 8(d)]. As expected, this order was in accordance with the observed strengths of the intermolecular interactions of the polymer/porphyrin system (Figures 3–6). That is, when the

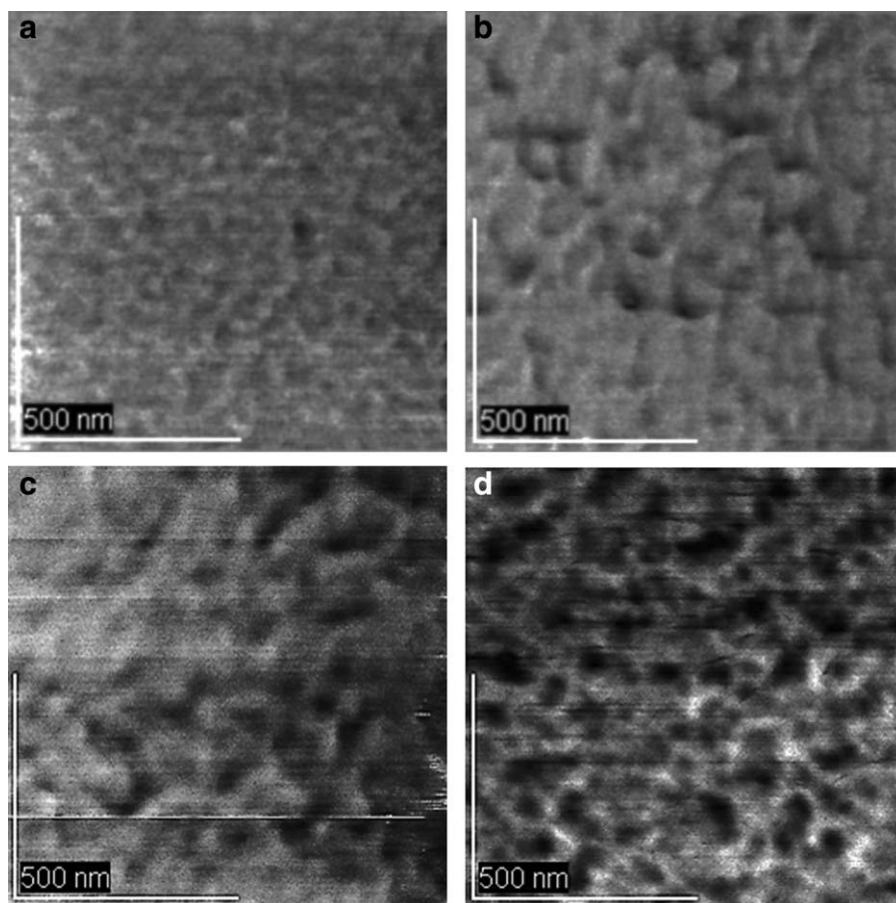


**Figure 8.** AFM images (phase mode) of the (a) 60/10/30 w/w PVNP/ZnTNpP/PCBM, (b) 60/10/30 PDAS/ZnTNpP/PCBM, (c) 60/10/30 PVPY/ZnTNpP/PCBM, and (d) 60/10/30 P3HT/ZnTNpP/PCBM blend thin films prepared from 10.0 mg/g chlorobenzene solutions.

intermolecular interactions of the polymer/porphyrin were considerable, such as in the combination of PVNP and ZnTNpP, the porphyrin/fullerene donor–acceptor complex was evidently dispersed in the polymer phase. In this case, intermixed domains appeared to form in the polymer thin film [Scheme 4(a)]. In contrast, when the polymer/porphyrin intermolecular interactions were not as strong, as was the case for the combination of P3HT and ZnTNpP, the distinct phase separation results and the porphyrin/fullerene donor–acceptor complex appeared to assemble at the borders between the polymer and fullerene phases [Scheme 4(b)].<sup>18</sup>

## CONCLUSIONS

The preparation, optical properties, and microphase separation of a series of semiconducting polymer (PVNP, PDAS, PYPY, and P3HT)/ZnTNpP/PCBM blend thin films were examined with the aim of realizing the controlled dispersion of porphyrin molecules in the films. The PVNP, PDAS, and PYPY used in this study were all synthesized by (living) anionic polymerization. The adjustment of the compatibility (i.e., intermolecular interactions) of the polymer/fullerene, polymer/porphyrin, and porphyrin/fullerene combinations was evidently an effective means of controlling the dispersion of porphyrin molecules throughout the semiconducting polymer thin films. The strength of the intermolecular interactions in the polymer/porphyrin system was found to decrease in the order PVNP/ZnTNpP > PDAS/ZnTNpP > PYPY/ZnTNpP > P3HT/ZnTNpP. The porphyrin/fullerene intermolecular interactions were quite strong compared with those of the polymer/fullerene and polymer/porphyrin systems, and the porphyrin/fullerene donor–acceptor complex readily formed in the semiconducting polymer thin films. When the intermolecular interactions of the polymer/porphyrin combination were enhanced, such as in the combination of PVNP and ZnTNpP, intermixed domains containing the porphyrin/fullerene donor–acceptor complex were formed in the polymer phase. In contrast, when the polymer/porphyrin intermolecular interactions were not as strong, as in the combination of P3HT and ZnTNpP, the porphyrin/fullerene donor–acceptor complex assembled at the borders between the polymer and fullerene phases. Therefore, the controlled dispersion of porphyrin molecules in the form of porphyrin/fullerene donor–acceptor complexes in semiconducting polymer thin films was achieved through the control of only the polymer/porphyrin intermolecular interactions. This concept may be applied to various combinations of porphyrin/fullerene systems in semiconducting polymer thin films to develop PSCs with excellent performance.

## REFERENCES

1. Maruyama, H.; Fujiwara, M.; Tanaka, K. *Chem. Lett.* **1998**, 27, 805.
2. Boyd, P. D. W.; Hodgson, M. C.; Rickad, C. E. F.; Oliver, A. G.; Chaker, L.; Brothers, P. J.; Bolskar, R. D.; Tham, F. S.; Reed, C. A. *J. Am. Chem. Soc.* **1999**, 121, 10487.
3. Konarev, D. V.; Neretin, I. S.; Slovokhotov, Y. L.; Yudanov, E. I.; Drichko, N. V.; Shul'ga, Y. M.; Tarasov, B. P.; Gumanov, L. L.; Batsanov, A. S.; Howard, J. A. K.; Lyubovskaya, R. N. *Chem. Eur. J.* **2001**, 7, 2605.
4. Yin, G.; Xu, D.; Xu, Z. *Chem. Phys. Lett.* **2002**, 365, 232.
5. Wang, Y. B.; Lin, Z. *J. Am. Chem. Soc.* **2003**, 125, 6072.
6. Xu, H.; Zheng, J. *Macromol. Chem. Phys.* **2010**, 211, 2125.
7. Castillo, U. J.; Guadarrama, P.; Fomine, S. *Org. Electron.* **2013**, 14, 2617.
8. Huang, C. S.; Wang, N.; Li, Y. L.; Li, C. H.; Li, J. B.; Liu, H. B.; Zhu, D. B. *Macromolecules* **2006**, 39, 5319.
9. Dastoor, P. C.; McNeill, C. R.; Frohne, H.; Foster, C. J.; Dean, B.; Fell, C. J.; Belcher, W. J.; Canipbell, W. M.; Officer, D. L.; Blake, I. M.; Thordarson, P.; Crossley, M. J.; Hush, N. S.; Reimers, J. R. *J. Phys. Chem. C* **2007**, 111, 15415.
10. Belcher, W. J.; Wagner, K. I.; Dastoor, P. C. *Sol. Energy Mater. Sol. Cells* **2007**, 91, 447.
11. Feng, J.; Zhang, Q.; Li, W.; Li, Y.; Yang, M.; Cao, Y. *J. Appl. Polym. Sci.* **2008**, 109, 2283.
12. Wang, C. L.; Zhang, W. B.; Horn, R. M. V.; Tu, Y.; Gong, X.; Cheng, S. Z. D.; Sun, Y.; Tong, M.; Seo, J.; Hsu, B. B. Y.; Heeger, A. J. *Adv. Mater.* **2011**, 23, 2951.
13. Cooling, N.; Burke, K. B.; Zhou, X.; Lind, S. J.; Gordon, K. C.; Jones, T. W.; Dastoor, P. C.; Belcher, W. J. *Sol. Energy Mater. Sol. Cells* **2011**, 95, 1767.
14. Lee, J. Y.; Song, H. J.; Lee, S. M.; Lee, J. H.; Moon, D. K. *Eur. Polym. J.* **2011**, 47, 1686.
15. Angiolini, L.; Benelli, T.; Cocchi, V.; Lanzi, M.; Salatelli, E. *React. Funct. Polym.* **2013**, 73, 1198.
16. Natori, I.; Natori, S.; Kanasashi, A.; Tsuchiya, K.; Ogino, K. *J. Polym. Sci. Part B: Polym. Phys.* **2013**, 51, 368.
17. Natori, I.; Natori, S.; Kanasashi, A.; Tsuchiya, K.; Ogino, K. *J. Appl. Polym. Sci.* **2013**, 128, 4212.
18. Natori, I.; Natori, S.; Hanawa, N.; Ogino, K. *J. Polym. Sci. Part B: Polym. Phys.* **2014**, 52, 743.
19. Shirakawa, E.; Yamasaki, K.; Hiyama, T. *J. Chem. Soc. Perkin Trans.* **1997**, 1, 2449.
20. Natori, I.; Natori, S.; Usui, H.; Sato, H. *Macromolecules* **2008**, 41, 3852.
21. Tanikawa, K.; Hirata, H.; Kusabayashi, S.; Mikawa, H. *Bull. Chem. Soc. Jpn.* **1969**, 42, 2406.
22. O'Malley, J. J.; Yanus, J. F.; Pearson, J. M. *Macromolecules* **1972**, 5, 158.
23. Rao, T. A.; Maiya, B. G. *Polyhedron* **1994**, 13, 1863.
24. Dixon, D. W.; Gill, A. F.; Giribabu, L.; Vzorov, A. N.; Alam, A. B.; Compans, R. W. *J. Inorg. Biochem.* **2005**, 99, 813.
25. Natori, I.; Natori, S.; Sekikawa, H.; Takahashi, T.; Ogino, K.; Tsuchiya, K.; Sato, H. *Polymer* **2010**, 51, 1501.